

Epigenetic Deregulation Across Chromosome 2q14.2 Differentiates Normal from Prostate Cancer and Provides a Regional Panel of Novel DNA Methylation Cancer Biomarkers

James Devaney^{1,2}, Clare Stirzaker^{1,2}, Wenjia Qu^{1,2}, Jenny Z. Song^{1,2}, Aaron L. Statham^{1,2}, Kate I. Patterson^{1,2}, Lisa G. Horvath^{2,3}, Bruce Tabor², Marcel W. Coolen^{1,2,4}, Toby Hulf^{1,2}, James G. Kench^{2,5}, Susan M. Henshall², Ruth Pe Benito², Anne-Maree Haynes², Regina Mayor^{6,7}, Miguel A. Peinado^{6,7}, Robert L. Sutherland², and Susan J. Clark^{1,2}

Abstract

Background: Previously, we showed that gene suppression commonly occurs across chromosome 2q14.2 in colorectal cancer, through a process of long-range epigenetic silencing (LRES), involving a combination of DNA methylation and repressive histone modifications. We now investigate whether LRES also occurs in prostate cancer across this 4-Mb region and whether differential DNA methylation of 2q14.2 genes could provide a regional panel of prostate cancer biomarkers.

Methods: We used highly sensitive DNA methylation headloop PCR assays that can detect 10 to 25 pg of methylated DNA with a specificity of at least 1:1,000, and chromatin immunoprecipitation assays to investigate regional epigenetic remodeling across 2q14.2 in prostate cancer, in a cohort of 195 primary prostate tumors and 90 matched normal controls.

Results: Prostate cancer cells exhibit concordant deacetylation and methylation of histone H3 Lysine 9 (H3K9Ac and H3K9me2, respectively), and localized DNA hypermethylation of *EN1*, *SCTR*, and *INHBB* and corresponding loss of H3K27me3. *EN1* and *SCTR* were frequently methylated (65% and 53%, respectively), whereas *INHBB* was less frequently methylated.

Conclusions: Consistent with LRES in colorectal cancer, we found regional epigenetic remodeling across 2q14.2 in prostate cancer. Concordant methylation of *EN1* and *SCTR* was able to differentiate cancer from normal ($P < 0.0001$) and improved the diagnostic specificity of *GSTP1* methylation for prostate cancer detection by 26%.

Impact: For the first time we show that DNA methylation of *EN1* and *SCTR* promoters provide potential novel biomarkers for prostate cancer detection and in combination with *GSTP1* methylation can add increased specificity and sensitivity to improve diagnostic potential. *Cancer Epidemiol Biomarkers Prev*; 20(1); 148–59. ©2011 AACR.

Authors' Affiliations: ¹Epigenetics Group and ²Cancer Research Program, Garvan Institute of Medical Research, Darlinghurst, NSW, Australia; ³Department of Medical Oncology, Sydney Cancer Centre, Royal Prince Alfred Hospital, Camperdown, NSW, Australia; ⁴Department of Human Genetics, Nijmegen Centre for Molecular Life Sciences, Radboud University Nijmegen Medical Centre, The Netherlands; ⁵Tissue Pathology and Diagnostic Oncology, Royal Prince Alfred Hospital and University of Sydney, Camperdown, NSW, Australia; ⁶Institut de Medicina Predictiva i Personalitzada del Càncer (IMPPC), Badalona, Catalonia, Spain; and ⁷Institut d'Investigació Biomèdica de Bellvitge (IDIBELL), L'Hospitalet, Catalonia, Spain

Note: Supplementary data for this article are available at Cancer Epidemiology, Biomarkers & Prevention Online (<http://cebp.aacrjournals.org>).

James Devaney, Wenjia Qu, Jenny Z. Song, and Clare Stirzaker contributed equally to the study.

Corresponding Author: Susan J. Clark, Epigenetic Research Laboratory, Cancer Program, Garvan Institute of Medical Research, 384 Victoria Street, Darlinghurst, NSW 2010, Australia. Phone: 61-2-92958315; Fax: 61-2-92958316. Email: s.clark@garvan.org.au

doi: 10.1158/1055-9965.EPI-10-0719

© 2011 American Association for Cancer Research.

Introduction

Prostate cancer is the most frequent nondermatologic malignancy in men worldwide and accounts for 10% of new male cancers (1, 2). The highest incidence rates of prostate cancer are in developed countries including the United States, Sweden, Canada, Switzerland, and Australia (3, 4) with worldwide deaths from prostate cancer being approximately 18 in 100,000 men (18 in 100,000 in the United Kingdom and Australia; 16 in 100,000 in the United States; and approximately 20 in 100,000 in Sweden, Switzerland, and the Netherlands; ref. 3). Well-established risk factors for the development of prostate cancer include age (5), race (6), family history (7), and geographic location (8, 9). Widespread screening using the prostate-specific antigen test (PSA) has led to an increased diagnostic rate and thus increased incidence of prostate cancer, with an associated decrease in mortality in recent years

(10). Although PSA is a highly sensitive serum test, its routine use has been a subject of continued controversy owing to its limited specificity (11, 12). Therefore, new markers are required to bolster the performance of PSA or modifications of PSA to improve the accuracy of prostate cancer detection.

It is now well recognized that deregulation of the cellular epigenetic pattern is a common and early event in carcinogenesis. Increased understanding of epigenetic modifications in carcinogenesis has led to new opportunities for the development of novel biomarkers for all cancers, including prostate cancer. Epigenetic mechanisms including aberrant DNA methylation and chromatin remodeling are known to be critical in the development and progression of prostate cancer (13–15). In particular, DNA hypermethylation of CpG-island-associated promoter regions of tumor-associated genes has frequently been reported, which has led to a greater focus on discovering genes that are silenced in prostate cancer via epigenetic deregulation (16). Notably hypermethylation of the glutathione *S*-transferase P1 (*GSTP1*) gene occurs in approximately 90% of all prostate cancers and is an early event, with DNA methylation lesions common in prostate intraepithelial neoplasia, making this gene a useful marker for early prostate cancer detection (17, 18). In addition to *GSTP1*, more than 40 genes have been reported to be targets of epigenetic gene silencing in prostate cancers (19) including adenomatous polyposis coli (*APC*), Ras association domain family 1A (*RASSF1A*), prostaglandin-endoperoxidase synthase 2 (*PTGS2*), multidrug resistance gene 1 (*MDR1*), retinoic acid receptor beta 2 (*RARβ2*), tazarotene-induced gene-1 (*TIG1*), and oestrogen receptor-beta (*ER-β*), which have also been shown to be involved in tumor initiation and progression and have been correlated with clinicopathologic parameters (20–25). A number of groups have also attempted to use combinations of genes to develop improved methylation-based tests for disease progression (26–28); however, no current epigenetic biomarker can predict disease aggressiveness or survival better than Gleason grade and serum PSA tests.

Typically, tumor-associated genes that are susceptible to promoter hypermethylation have been identified using an individual candidate gene approach. Recently, however, we have shown that gene silencing and DNA hypermethylation can occur across large regions of the chromosome and in combination with histone H3 lysine 9 dimethylation (H3K9me2) can suppress the expression of neighboring genes, including genes that may not contain a promoter-associated CpG island, by a process termed long-range epigenetic silencing (LRES; ref. 29). We have previously shown that gene expression across the 4-Mb chromosomal region 2q14.2 is commonly suppressed in colorectal cancer and this is associated with aberrant DNA and histone methylation (29). Moreover, a hypermethylated gene in the 2q14.2 region, *Engrailed-1* (*EN1*), is a useful diagnostic marker in stool and serum DNA samples in colorectal cancer patients (30). The aim of this

study was to investigate the epigenetic state of the 2q14.2 region in prostate cancer and to determine the potential of aberrant methylation of genes within the region in prostate cancer diagnosis and prognosis.

Materials and Methods

Cell culture conditions

Human prostate cancer cell lines LNCaP, PC-3, and DU145 were obtained from American Type Culture Collection. LNCaP prostate cancer cells were cultured in T-medium with 10% heat-inactivated FCS and 1% penicillin/streptomycin (Invitrogen), as described previously (31). The cells were grown at 37°C in 5% CO₂ atmosphere and split 1:3 every 4 to 5 days. DU145 and PC-3 prostate cancer cells were grown in RPMI medium with 10% FBS. Normal prostate epithelial cells (PrEC; Cambrex Bio Science Cat. No. CC-2555; Tissue acquisition 13683 and 13639), were cultured and subcultured according to the manufacturer's instructions in Prostate Epithelial Growth Media (PrEGM Cambrex Bio Science Cat No CC-3166). Cell lines were authenticated by short tandem repeat polymorphism, single nucleotide polymorphism, and fingerprint analyses, and passaged for less than 6 months.

5-Aza-2'-deoxycytidine and trichostatin A treatment of cells

The prostate cancer cell line LNCaP was seeded at 0.5×10^6 cells. The cells were treated 24 hours later with 0.5 or 3 mmol/L 5-aza-2'-deoxycytidine (5-Aza-dC; Sigma) for 24 hours and cultured with fresh medium for another 48 hours. Cells were treated with 100 nmol/L trichostatin A (TSA; Sigma) for 24 hours. For cotreatment of cells with 5-Aza-dC and TSA, 5-Aza-dC was added initially for 24 hours, after which it was removed and TSA added for an additional 24 hours.

RNA extraction and Quantitative Real-Time RT-PCR

RNA was extracted from PrEC and LNCaP cell lines using Trizol reagent (Invitrogen) and cDNA was reverse transcribed from 2 μg of total RNA using SuperScript III RNase H-Reverse Transcriptase (Invitrogen Life Technologies), according to the manufacturer's instructions. The reaction was primed with 200 ng of random hexamers (Roche). The reverse transcription reaction was diluted 1:20 with sterile H₂O before addition to the RT-PCR. Expression was quantified using a fluorescent real-time detection method using the ABI Prism 7000 Sequence Detection System. Reverse transcription reaction (5 μL) was used in the quantitative real-time PCR reaction using 2x SYBR Green 1 Master Mix (P/N 4309155) with 50 ng of each primer. The primers used for amplification are listed in Supplementary Table S1. To control for the amount and integrity of the RNA, the Human 18S ribosomal RNA (rRNA) kit (P/N 4308329; Applied Biosystems), containing the rRNA forward and reverse primers and rRNA VICTM probe, was used. Reverse transcription (5 μL) was

used in a 20 μ L reaction in TaqMan Universal PCR Master Mix (P/N 4304437) with 1 μ L of the 20 \times Human 18S rRNA mix. The reactions were performed in triplicate and the SD was calculated using the Comparative method (ABI PRISM 7900 Sequence Detection system User Bulletin #2, 1997 P/N 4303859). The cycle number corresponding to where the measured fluorescence crosses a threshold is directly proportional to the amount of starting material. The mean expression levels are represented as the ratio between each gene and 18S rRNA expression.

Chromatin immunoprecipitation (assays)

Chromatin immunoprecipitation (ChIP) assays were carried out as previously described (32) according to the manufacturer's instructions (Upstate Biotechnology). The complexes were immunoprecipitated with antibodies specific for acetylated-histone H3 (#06-599), dimethyl-histone H3(lys9) (#07-441), or trimethyl-histone H3 (lys27) (#07-449; all from Millipore). No-antibody controls were also included for each ChIP assay with no precipitation being observed. Complexes were collected by salmon sperm DNA/protein A agarose slurry and washed several times. The amount of target immunoprecipitated was measured by real-time PCR using the ABI PRISM 7900HT Sequence Detection System. Amplification primers are listed in Supplementary Table S1. Reactions of 20 μ L were set up using the TaqMan Universal PCR Master Mix (2 \times) in a 396-well plate. Four microliters of immunoprecipitated DNA, no-antibody control, or input chromatin were used in each PCR and the PCRs were set up in triplicate. Universal thermal cycling conditions were used: 50°C for 2 minutes, then 95°C for 10 minutes, followed by 95°C for 15 seconds and 60°C for 1 minute repeated for 40 cycles. For each sample, an average Ct value was obtained for immunoprecipitated material and for the input chromatin. The difference in Ct values (delta Ct) reflects the difference in the amount of material that was immunoprecipitated relative to the amount of input chromatin and this was then expressed relative to the Ct value for LNCaP (ABI PRISM 7900 Sequence Detection system User Bulletin #2, 1997 (P/N 430385)).

Real-time PCR heat dissociation melt curve analysis

Following completion of seminested bisulfite PCR, 0.4 μ L of 10 \times SYBR Green I nucleic acid gel stain (P/N 4309155) was added to the PCR reaction following completion. Nested bisulfite PCR primers are listed in Supplementary Table S2. The PCR reactions were cycled at 95°C for 15 seconds, 60°C for 20 seconds, with the temperature increasing gradually from 60°C to 90°C and the melting dissociation trace was analyzed on the ABI Prism 7900HT Sequence Detection System. CpGenome Universal Methylated Control DNA (Chemicon International Inc., Cat#S7821) was used as a positive control to amplify fully methylated DNA. Human genomic DNA (Roche Cat#1169112001) was used as a positive control to amplify fully unmethylated DNA.

Prostate samples

Radical prostatectomy samples were retrospectively identified (with Gleason grades of 3, 4 or 5), with matched normal prostate tissue where available, from a cohort of archival formalin-fixed, paraffin-embedded specimens selected from the previously described group of 732 patients (33). Tissue blocks were reviewed by a pathologist (James G. Kench) and 195 cases (90 with matched normal samples) had >50% tumour present in the specimen. All patients had undergone radical prostatectomy for clinically localized prostate cancer at St. Vincent's Private Hospital, Sydney, Australia (Human Research Ethics Committee Approval H00/088). Patients were followed postoperatively by their surgeons on a monthly basis until satisfactory urinary continence was obtained and then at 3-month intervals until the end of the first year, at 6-monthly intervals to 5 years and yearly thereafter. Relapse was defined by the following criteria: biochemical disease progression with a serum PSA concentration at or above 0.4 ng/mL rising over a 3-month period or local recurrence on digital rectal examination confirmed by biopsy or by subsequent rise in PSA. Clinical and pathologic data were collected and data-based for 194 patients.

DNA extraction and bisulfite conversion

Cores from representative blocks were deparaffinized and DNA was extracted using the Puregene kit (Qiagen) using standard procedures. Bisulfite modification was carried out as previously described (34) and incubated for 4 hours at 55°C with sodium metabisulfite prior to desulfonation.

Methylation-specific headloop suppression PCR

Methylation-specific headloop suppression PCR (MSH-PCR) primers and probes were developed for *EN1*, *SCTR*, *INHBB* (Supplementary Table S2), and *GSTP1* (35). The headloop primer consists of a base primer specific for bisulfite-treated DNA, with an attached sequence of bases at the 5' end, the headloop (Supplementary Fig. S1). The headloop moiety is specific for bisulfite-treated unmethylated DNA and acts to suppress amplification of unmethylated DNA (35) and a targeted fluorescent probe specifically detects the amplified and methylated DNA.

Primer sequences and probes (Integrated DNA technologies) are documented in Supplementary Table S2. *EN1*, *SCTR*, *INHBB*, and *GSTP1* headloop real-time PCR was carried out using the ABI 7900 (AME Bioscience). Standard PCR conditions for real-time PCR (in 15 μ L) were 2 mmol/L MgCl₂, 0.2 mmol/L of each dNTP, 200 nmol/L primers, 100 nmol/L probes, and 0.1 units platinum *Taq* DNA polymerase (Invitrogen). Standard cycling conditions were 95°C for 120 seconds, then 50 cycles at 95°C for 15 seconds and 60°C for 60 seconds. Specific annealing temperatures and optimum magnesium concentrations for each gene are shown in Supplementary Fig. S1. PCR was performed in separate wells for each primer and

probe set and each sample was run in triplicate. Negative controls and water controls together with positive controls for standard curve generation were included in each experiment. Sodium bisulfite-treated CpG-methylated (CpGenome Universal methylated DNA, Millipore) and human genomic (Roche diagnostics) DNA were used for the sensitivity and specificity assays.

MALDI-TOF mass spectrometry DNA methylation analysis

Primers were designed to interrogate the CpG island surrounding the promoter of *EN1*, *SCTR*, and *INHBB* are tabulated in Supplementary Table S1. Experimental conditions were as described previously (36).

Statistical analysis

The receiver operating characteristic (ROC) curve and the respective area under the curve (AUC) were calculated for each gene to assess the potential for promoter methylation to differentiate prostate cancer from normal tissue. Fisher's exact, χ^2 , and McNemar's tests were calculated using the STATA 9 package. Disease-specific relapse was measured from the date of radical prostatectomy (RP) to the date of last follow-up. Kaplan-Meier and log-rank analyses evaluating disease relapse were performed. Further survival analysis was performed using univariate and multivariate analyses in a Cox proportional hazards model for *GSTP1* status and other clinical and pathologic predictors of outcome as previously described (37). The multivariate model was produced by assessing *GSTP1* status with other baseline covariates of clinical relevance such as Gleason grade, pathologic stage, and preoperative PSA, which were modeled as dichotomous or continuous variables as appropriate. All reported *P* values are 2-sided. All statistical analyses were performed using Statview 4.5 software (Abacus Systems).

Results

Epigenetic associated gene suppression occurs across 2q14.2 in prostate cancer cells

To determine whether concordant gene suppression occurs across 2q14.2 in prostate cancer cells we used RT-qPCR to measure mRNA expression levels of 10 genes in the 4-Mb region spanning 2q14.2 (Fig. 1A) in both normal prostate cells, PrEC, and the prostate cancer cell line, LNCaP (Fig. 1B). We used microarray analysis to compare mRNA expression in PrEC cells with expression in the prostate cancer cell lines LNCaP, PC3, and DU145 (Supplementary Fig. S2), and average expression of each gene in 13 tumor-matched normal samples (ref. 38; Fig. 1C). Of the 10 genes analyzed, 8 have CpG-island-associated promoters (*DDX18*, *INSIG2*, *EN1*, *SCTR*, *PTPN4*, *RALB*, *INHBB*, *TSN*), 1 has a CpG island located at the 3' end of the gene (*GLI2*), and *MARCO* has no associated CpG island. We found there was an overall suppression of gene expression across 2q14.2 between the prostate cancer cell lines and normal PrECs, and between

primary tumor samples and matched normal tissue (Fig. 1B and C), with over half the genes in the region (*EN1*, *MARCO*, *SCTR*, *PTPN4*, *INHBB*, *GLI2*) already expressed at low or basal levels in the normal prostate cells. Reduction of gene expression was commonly found for the remaining genes (*DDX18*, *INSIG2*, *RALB*, and *TSN*) in both tumor cell lines and primary tumor samples.

To determine whether the general reduction in gene expression across the 2q14.2 region in the prostate cancer cells was related to a change in DNA methylation or repressive chromatin modification, we treated LNCaP cells with either demethylating 5-Aza-dC alone or in combination with the histone deacetylase inhibitor TSA. As a control for these treatment conditions, we tested expression changes for *GSTP1*, which is known to be methylated and deacetylated in LNCaP cells (39). We found using RT-qPCR that, as for *GSTP1*, *EN1*, and *INHBB* were also strongly re-expressed after treatment with 5Aza-dC alone and *SCTR* with a combination of 5Aza-dC and TSA treatment (Fig. 1D), suggestive of DNA hypermethylation and repressive chromatin at promoter-associated CpG islands in these genes. In contrast to colorectal cancer cells (30), *DDX18*, *INSIG2*, *PTPN4*, *MARCO*, *RALB*, *GLI2*, and *TSN* showed minimal or no reexpression after treatment with 5-Aza-dC and TSA indicating that either these genes may not be epigenetically controlled or that prostate cells are not permissive for their expression. Expression of each of the 10 genes across 2q14.2 did not change in the normal prostate cell line PrEC following treatment with 5-Aza-dC (Supplementary Fig. S3).

Epigenetic remodeling of 2q14.2 genes in prostate cancer cells

To further investigate whether the CpG-island-associated genes spanning the 2q14.2 region were hypermethylated in prostate cancer, normal prostate and cancer cell line DNA were bisulfite treated, PCR amplified, and the methylation of the CpG-island-associated genes was analyzed by PCR heat dissociation melt curve analysis (40, 41). All the genes analyzed were unmethylated in PrEC cells, and 3 genes, *EN1*, *SCTR*, and *INHBB* were methylated in LNCaP cells (Fig. 1E); a finding consistent with reexpression after either 5-Aza-dC or a combination of 5-Aza-dC and TSA treatment. In addition, *EN1* and *SCTR* were also methylated in the prostate cancer cell lines PC-3 and DU145 (data not shown).

To determine whether the general gene suppression across the 2q14.2 region was associated with chromatin remodeling, we analyzed active (H3K9Ac) and repressive (H3K9me2 and H3K27me3) histone modifications associated with the 10 gene promoter regions. The chromatin from PrEC and LNCaP cells was immunoprecipitated (ChIP) and quantified by qPCR. In PrEC cells, all 10 genes were associated with H3K9Ac and this mark was concordantly lost in LNCaP cells,

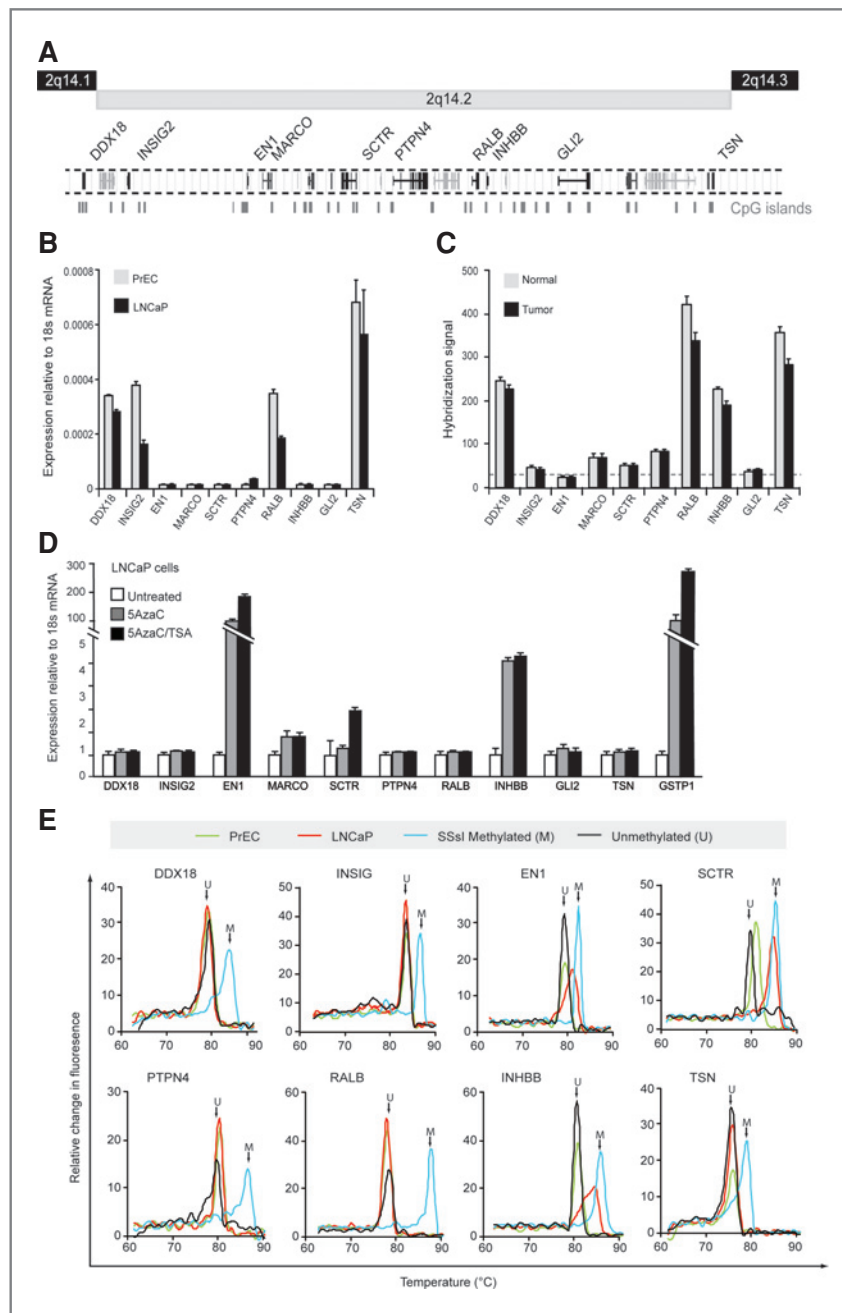


Figure 1. Gene expression and effect of 5-AzaC and TSA on gene expression across region 2q14.2 in prostate cancer. **A**, chromosomal location of the analyzed genes across 2q14.2 on chromosome 2. **B**, mRNA expression levels of the genes across 2q14.2 in normal prostate epithelial cells (PrEC) was compared with expression in the prostate cancer cell line LNCaP. cDNA was prepared from RNA isolated from the cells lines and quantified by RT-PCR. The expression of each gene was measured relative to the expression of 18s rRNA. Error bars represent the SEM of 3 individual reactions. **C**, average expression of the 10 genes across 2q14.2 from 13 matched normal and tumor samples. 26 arrays (13 matched normal/tumor Gleason score 6–8; ArrayExpress E-TABM-26; ref. 38) were downloaded. All probes were preprocessed using Robust Multichip Analysis (RMA) and median normalization was applied per gene with a cutoff value of 32 (or $\log_2 < 5$; dashed line) in raw signal measurement values. The average hybridization signal of the 13 tumor and 13 matched normal samples is plotted. Error bars represent SEM. **D**, RNA was isolated from untreated LNCaP cells and LNCaP cells that were treated with 5-AzaC, TSA, or a combination of 5-AzaC and TSA. RNA was reverse transcribed, and expression was quantitated by real-time qPCR and normalized to 18s rRNA expression. Expression of control gene *GSTP1* is shown and expression is shown relative to the untreated control. Error bars represent the SEM of at least 3 individual reactions. **E**, DNA from LNCaP and PrEC cells was isolated, bisulfite treated and bisulfite DNA-specific primers were used to amplify promoter-associated CpG-island regions of the genes. Melting dissociation temperature was then observed for each gene and its methylation status was determined (M, methylated; U, unmethylated). CpGenome Universal Methylated Control DNA was used as a positive control to amplify fully methylated DNA for the dissociation curve and Human genomic DNA was used as a positive control to amplify fully unmethylated DNA for the dissociation curve. The melting dissociation curves for *EN1*, *SCTR*, and *INHBB* shifted toward that of the fully methylated control, indicative of methylation of these genes in these samples.

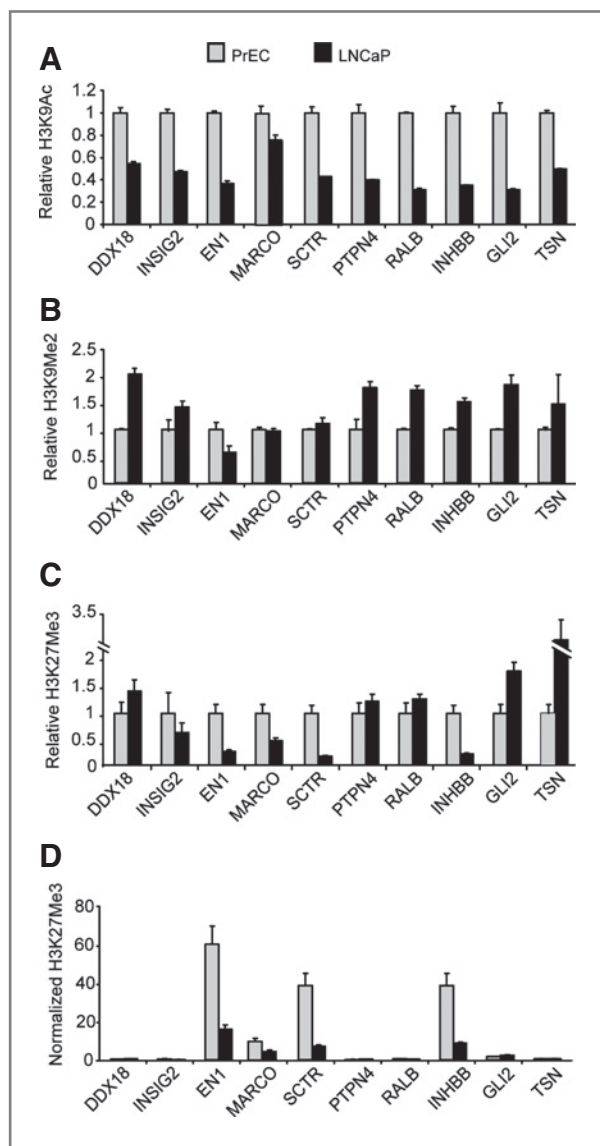


Figure 2. Chromatin immunoprecipitation (ChIP) across the 2q14.2 region. Chromatin from LNCaP and PrEC cells was immunoprecipitated with acetylated histone H3K9 (A), dimethylated histone H3K9 (B), and trimethylated histone H3K27 (C and D) antibodies. The amount of immunoprecipitated target was quantified by real-time PCR and plotted as the ratio of immunoprecipitated DNA to input (A) or 16-Cen (B–D; ref. 62) and then made relative to PrEC. Absolute levels of trimethylated histone H3K27 binding is also shown in D as relative to 16-Cen, indicating the relative enrichment in *EN1*, *SCTR*, and *INHBB*.

indicating a general deacetylation of the 2q14.2 region in the cancer cells (Fig. 2A). In addition, there was an overall modest increase in binding of the repressive chromatin mark H3K9me2 in LNCaP cells relative to PrEC cells across the region with the exception of *EN1*, *MARCO*, and *SCTR* (Fig. 2B). Changes in H3K27me3 were also observed with both gain and loss of the polycomb mark in LNCaP cells (Fig. 2C). Most notable was the loss of H3K27me3 binding to *EN1*, *MARCO*,

SCTR, and *INHBB* in LNCaP cells compared with binding in PrECs (Fig. 2D). Interestingly, the CpG-island-associated genes *EN1*, *SCTR*, and *INHBB* were also DNA hypermethylated in LNCaP cells (Fig. 1E), consistent with the finding that genes methylated in cancer are often marked by H3K27me3 in the normal cell (42).

DNA methylation analysis using MALDI-TOF mass spectrometry and methylation-specific headloop PCR

We used quantitative MALDI-TOF mass spectrometry (36) to map in further detail the methylation status of sequential CpG dinucleotides in the 250 to 400 base pair (bp) regions spanning the CpG-island promoters of *EN1*, *SCTR*, and *INHBB*. Normal prostate PrEC cells and blood DNA were unmethylated for each of the genes analyzed, whereas the CpG-island promoter regions associated with *EN1*, *SCTR*, and *INHBB* were methylated to various degrees in LNCaP, DU145, and PC-3 cells (Fig. 3A and B). To investigate the frequency of methylation in clinical samples, we developed more sensitive MSH-PCR assays for *EN1*, *SCTR*, and *INHBB* (Supplementary Fig. S1A–C). A MSH-PCR assay for the *GSTP1* gene was also used to compare for differential methylation in normal and cancer tissues (35). The sensitivity and specificity of each MSH-PCR assay was optimized to detect picogram amounts of methylated DNA in a background of unmethylated DNA. Primer and probe design, coupled to PCR optimization, permitted detection of as little as 10 to 25 pg of methylated DNA for all MSH-PCR assays, with a PCR efficiency of approximately 85% and a specificity of at least 1:1,000 (Supplementary Fig. S1B).

DNA methylation of *EN1*, *SCTR*, and *INHBB* in primary prostate cancer

To determine the frequency of *EN1*, *SCTR*, and *INHBB* methylation in clinical samples, we used MSH-PCR to survey 195 prostate cancers from FFPE tissue from radical prostatectomy patients, 90 of whom had matched normal samples and 194 of which had known biochemical relapse (Table 1). We found that *EN1* was methylated in 127 of 195 (65%) and *SCTR* was methylated in 104 of 195 (53%) radical prostatectomy specimens (Fig. 4A). However, we found that *INHBB* was only minimally methylated in 5 of 65 (7.7%) of the cancers; 5 of 24 in tumors without matched normal (data not shown), and 0 of 41 in tumors with matched normal (Fig. 4B and C). Methylation of *GSTP1* was used as a control and was methylated in 172 of 195 (88%) of the prostate cancers (Fig. 4A). Concordant methylation of *EN1* and *SCTR* ($P < 0.0001$), and concordant methylation of *EN1*, *SCTR*, and *GSTP1* ($P < 0.0001$) was also observed (Fig. 4A). Of the 23 prostate cancer samples that did not show *GSTP1* methylation, 6 (26%) were methylated for *EN1* and 3 (13%) were methylated for *SCTR*.

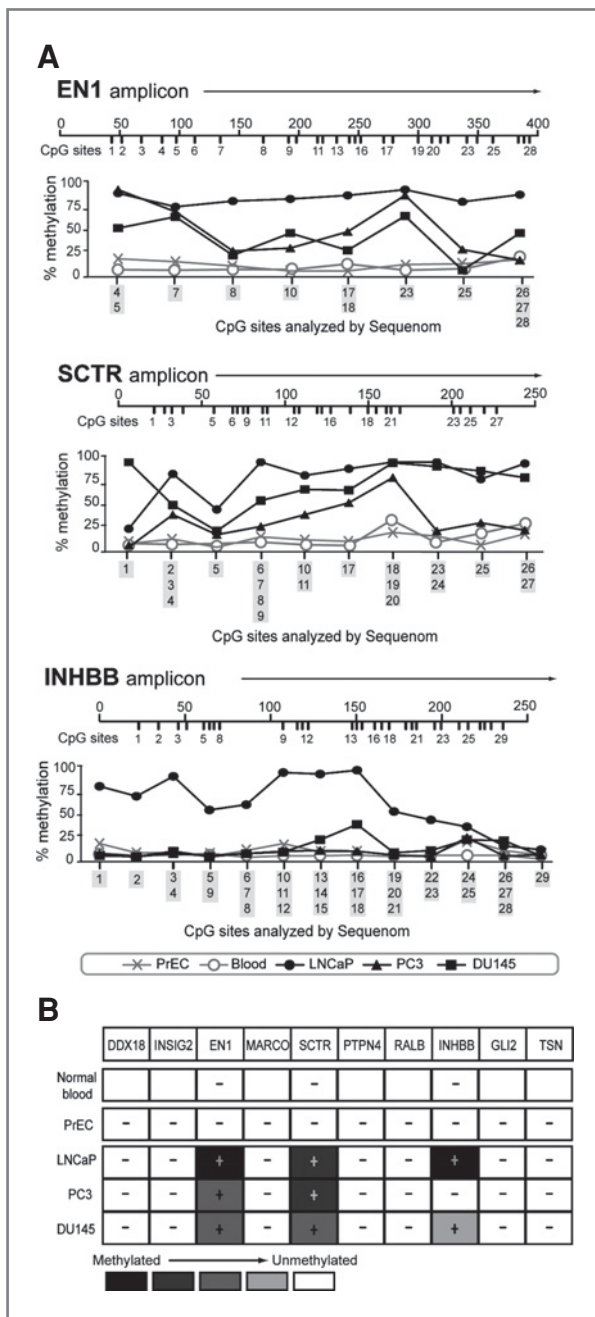


Figure 3. MALDI-TOF mass spectrometry DNA methylation analysis of prostate cancer cell lines. **A**, percent methylation for each CpG unit across the CpG-island promoter regions of *EN1*, *SCTR* and *INHBB* were plotted for normal prostate epithelial cells (PrEC), normal blood DNA (Roche), LNCaP, PC3, and DU145 cells. **B**, overall summary of the methylation profile for the gene promoters within 2q14.2. All genes tested are unmethylated in PrEC cells and blood DNA (white boxes) whereas *EN1*, *SCTR*, and *INHBB* are variably methylated (grey boxes). Open boxes, not determined. Percent methylation was summarized into 100% to 0% (black to white greyscale boxes) based on the average of CpG unit methylation.

Table 1. Prostate cancer patient cohort ($n = 194$)

Mean age (range)	63 y (49-75)
Gleason Score	
≤6	81 (42%)
7	70 (36%)
8-10	42 (22%)
P stage	
PT2	90 (47%)
PT3/4	104 (53%)
EPE	
Yes	94 (48%)
No	100 (52%)
SVI	
Yes	39 (20%)
No	155 (80%)
Margins	
Positive	111 (57%)
Negative	83 (43%)
Median F/U	109 months (12-193)
Relapse	121/194 (62%)

Concordant *EN1*, *SCTR*, and *GSTP1* methylation in prostate cancer improves diagnostic potential and *GSTP1* methylation is associated with a longer time to relapse

Similar to *GSTP1*, DNA methylation of *EN1* and *SCTR* could significantly ($P < 0.0001$) differentiate prostate cancer from adjacent normal tissue (Fig. 4B). We found, however, that for the DNA samples that did contain methylation in the adjacent normal tissues, the amount of methylated normal DNA was greatly reduced (Fig. 4C; Supplementary Fig. S4), indicating that the methylated DNA was possibly due to cancer cell contamination in the normal samples or potentially a field effect on the prostate gland (43). A well-established method for diagnostic biomarker analysis is the ROC curve, a plot of sensitivity versus specificity. A ROC curve was generated by plotting the fraction of true positives (cancer) versus the fraction of false positives (normal); the AUC is then used as a measure of accuracy of the test. We included all the normal samples that were positive for methylation, regardless of the absolute amount of methylated DNA detected. Because a number of positive normal specimens had a greatly reduced amount of methylated DNA relative to matched normal (Fig. 4C; Supplementary Fig. S4) it is likely that these were false positives. We found an improvement in the potential diagnostic use of *GSTP1* DNA methylation (17) when combining it with the concordant methylation of 2q14.2 genes, *EN1* and *SCTR*. This improved the AUC from 0.907 (*GSTP1* only) to 0.940 (*GSTP1*, *EN1*, *SCTR*; Fig. 5A).

We next investigated whether DNA methylation of the *EN1*, *SCTR*, and *GSTP1* promoter regions was correlated to any of the established prognostic clinicopathologic parameters including Gleason Score, pathologic stage,

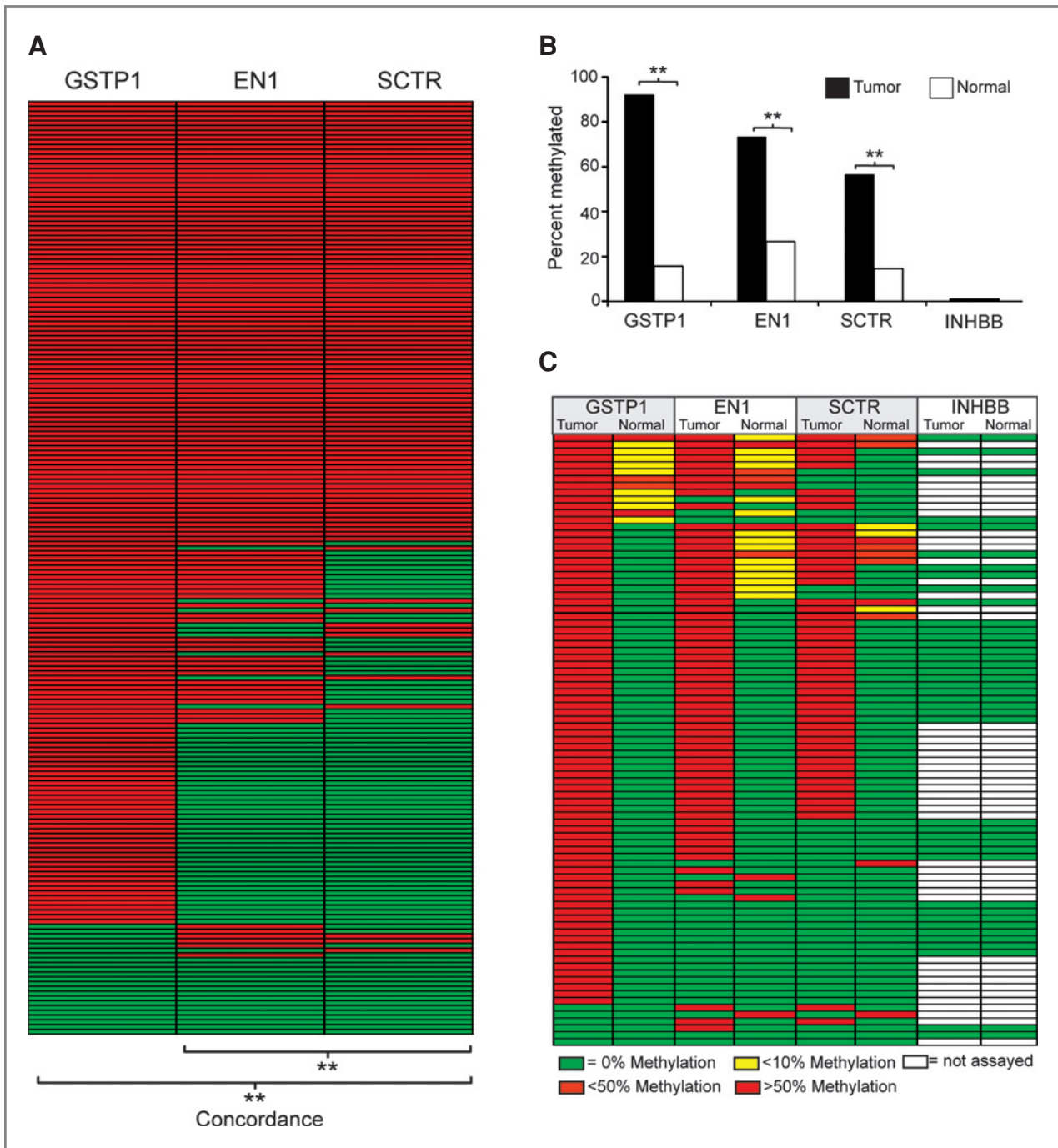


Figure 4. Methylation profiles of matched normal and prostate cancer samples. **A**, DNA methylation status of *EN1*, *SCTR*, and the control gene *GSTP1* in 195 prostate tumor samples classified according to Gleason score (G3–G5). Red boxes are methylated; green boxes are unmethylated. *EN1* and *SCTR* were frequently methylated in prostate cancers in a concordant fashion ($P < 0.0001$) and were methylated in a concordant fashion with *GSTP1* ($P < 0.0001$). **B**, tumor and matched normal samples analyzed by McNemar's paired test. *GSTP1* ($n = 90$, $P < 0.0001$), *EN1* ($n = 90$, $P < 0.0001$), and *SCTR* ($n = 90$, $P < 0.0001$) could all distinguish cancer from normal tissue. *INHBB* ($n = 41$) showed no methylation in either tumor or matched normal samples and so *INHBB* methylation analysis was not extended to the rest of the cohort. **C**, methylation of *GSTP1*, *EN1*, *SCTR*, and *INHBB* in matched normal and cancer samples. Methylated samples are shown as red, unmethylated as green, normal samples with less than 10% methylation are shown as yellow, less than 50% as orange, and more than 50% as red.

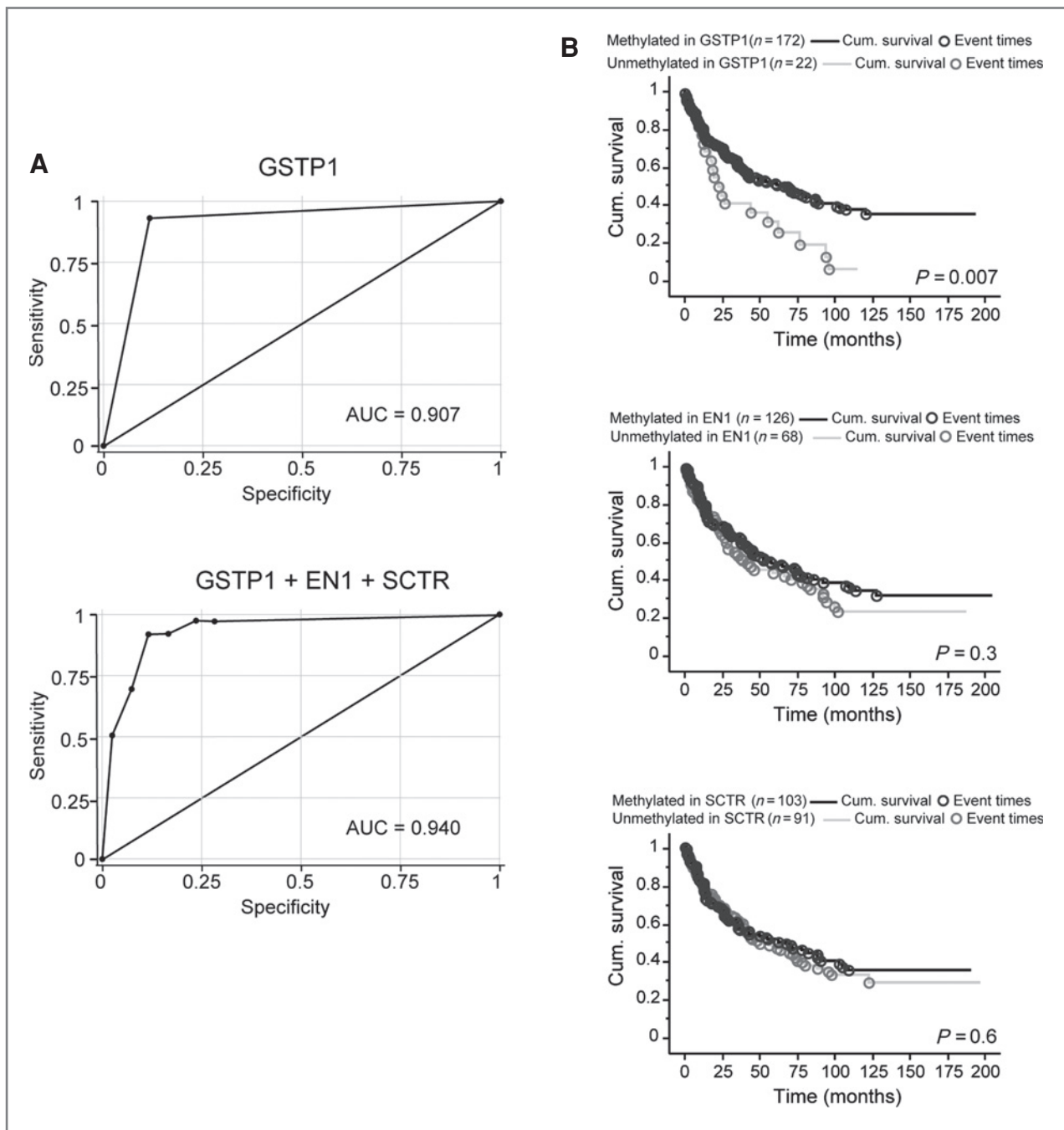


Figure 5. Receiver operating curves and Kaplan–Meier analysis. A, *GSTP1* promoter methylation prediction of diseased tissue gives an area under the curve (AUC) of 0.9070. Combining *GSTP1* with *EN1* and *SCTR* improves the accuracy of the test using *GSTP1* only, and gives an AUC of 0.940. B, Kaplan–Meier analysis was used to generate graphs that represent time to biochemical relapse versus DNA methylation of *GSTP1*, *EN1*, and *SCTR*.

seminal vesicle involvement (SVI), margins positive, extra-prostatic extension (EPE), and preoperative PSA. Methylation data on the 3 genes were available on 194 men with localized prostate cancer treated with radical prostatectomy. The cohort had a median follow-up of 109 months (range, 12–193 months) with a 62% biochemical relapse rate. This was a high-risk cohort of patients

with a 22% Gleason score 8 to 10 and quite a high relapse rate (Table 1). There was no correlation (data not shown) between methylation patterns of *EN1* and *SCTR* promoters and Gleason Score, pathologic stage, SVI, EPE, and preoperative PSA levels. In addition, there was no association with methylation of *EN1* or *SCTR* and time to relapse (Fig. 5B). In contrast, we noted that methylation of

GSTP1 was associated with a longer time to relapse compared with patients who do not have methylated *GSTP1* ($P = 0.007$, Fig. 5B). Furthermore, on multivariate analysis, methylation of *GSTP1* ($P = 0.01$) was an independent predictor of outcome when modeled with Gleason score ($P = 0.07$), preoperative PSA ($P = 0.003$), margin status ($P = 0.09$), and pathologic stage ($P = 0.3$; Supplementary Table S3). ECE and SVI were not included in the final multivariate analysis as they are incorporated as part of the pathologic stage.

Discussion

We previously reported that gene expression across chromosome 2q14.2 was commonly suppressed in colorectal cancer by LRES (29) and genes within these regions could be important biomarkers for colorectal cancer detection (30). In this study we show that chromosome 2q14.2 is also epigenetically remodeled in prostate cancer cells, resulting in a consolidation of gene inactivity and reduction in gene plasticity by LRES (44). Moreover, we find that gene-specific aberrant DNA methylation in 2q14.2 differentiates prostate cancer from normal prostate cells and provides diagnostic potential, but unlike *GSTP1* methylation, 2q14.2 gene methylation is not significantly associated with a longer disease-free period.

Interestingly, 2q14.2 genes are commonly associated with the histone H3K9Ac active modification mark in normal prostate cells, even though many of the genes in this region are not expressed or expressed only at basal levels. We find that the low level of gene expression observed in the LNCaP prostate cancer cell line across the 2q14.2 region corresponds with a concordant loss of H3K9Ac and gain of H3K9me2. DNA methylation analysis revealed that similar to colorectal cancer there is also a significant increase in the frequency of DNA hypermethylation of specific genes in prostate cancer within the 2q14.2 region, even though these genes were already inactive in the normal prostate epithelial cells. Specifically, the promoter-associated CpG island of genes *EN1*, *SCTR*, and *INHBB* exhibited increased DNA methylation in prostate cancer cell lines compared with the normal prostate cell line PrEC, and *EN1* and *SCTR* were found to be significantly methylated in clinical prostate cancer cells. The *EN1* gene codes for a homeobox transcription factor, which interacts with the WNT signaling pathway (45) and is essential for development (46). *SCTR* encodes the secretin receptor, a G-protein-coupled receptor that is also hypermethylated and downregulated in pancreatic (47) and colorectal cancer (29). The *INHBB* gene encodes the inhibin β subunit of the signaling hormone/growth factor inhibin. *INHBB* is involved in cell differentiation and proliferation (48) and is downregulated in breast cancer (49). A tumor suppressor role of these genes in prostate cancer is unlikely as we show that they are normally only expressed at low or basal levels in prostate epithelial cells. However, our results suggest that aberrant methylation of *EN1*, *SCTR*, and *INHBB* in prostate cancer is more likely to

be associated with the fact that these genes are marked by the polycomb group protein H3K27me3 in normal prostate epithelial cells, which is then replaced by DNA methylation in LNCaP cells, consistent with the finding that genes that are commonly methylated in cancer are often marked by H3K27me3 in the embryonic stem cells (42, 50, 51). However, the underlying mechanism associated with the exchange of epigenetic marks in cancer cells is not well understood, especially as loss of H3K27me3 marked genes in cancer cells occurs even though the H3K27 methylase EZH2 levels are often increased in metastatic prostate cancer (52, 53).

GSTP1, which encodes an enzyme involved in intracellular detoxification reactions, is also commonly methylated in prostate cancer and is the gold standard epigenetic marker for prostate cancer detection (17). However, unlike the 2q14.2 genes destined for cancer methylation, *GSTP1* CpG-island promoter is not marked by H3K27me3 in PrEC cells, but gains DNA methylation independently of H3K27me3 through 5MeC reprogramming (21, 54). Interestingly, even though *GSTP1* is commonly methylated, there are approximately 10% of prostate cancers where *GSTP1* remains unmethylated and what is not yet clear is whether the predictive value of a negative test is sufficient to change the course of medical care (21). Consistent with previous reports (55), we show that patients that are negative for *GSTP1* methylation have a poorer prognosis, suggesting that these cancers may have originated by a different pathway or possibly from an earlier cancer progenitor stem cell.

To determine whether hypermethylation of the 2q14.2 genes (*EN1*, *SCTR*, and *INHBB*) could improve prostate cancer detection where *GSTP1* is unmethylated, we developed sensitive, high-throughput DNA methylation assays. Because a common problem associated with long-term storage of biological material is sample degradation, we designed the MSH-PCR assays to amplify small (100 bp) amplicons from bisulfite-converted DNA isolated from FFPE tissue. MSH-PCR has advantages over many other high-throughput methylation assays as it is based on suppression of the unmethylated DNA and amplification of low levels of methylated DNA and unlike MSP assays, does not rely on design of primers with CpG methylation in the 3' end of the primer sequence (35). Using these assays we found that the methylation state of *EN1*, *SCTR*, and *GSTP1*, both individually and concordantly, could differentiate tumor from normal tissue ($P < 0.0001$). Interestingly in the 23 of 195 (12%) of prostate cancer samples that did not show *GSTP1* promoter methylation, 26% were methylated for *EN1*, 13% for *SCTR*, and 9% for both *EN1* and *SCTR* suggesting that some 2q14.2 methylation changes may also occur early in carcinogenesis, as is suggested for *GSTP1* (13). In fact, using ROC curve analysis we found the diagnostic accuracy of *GSTP1* DNA methylation could be improved by combining it with methylation of *EN1* and *SCTR* from the 2q14.2 region to form a potential new marker panel for prostate cancer detection.

Finally, in addition to *GSTP1* methylation marks, there is a growing collection of candidate-hypermethylated single gene loci that also appear to function well when combined as cancer DNA surrogates, including *APC*, *RASSF1a*, and *MDR1* (56–58). However, unlike detection of prostate cancer DNA using tests for methylation marks, DNA methylation biomarkers for prostate cancer prognosis are still limited. Methylation marks for *EDNRB*, *RAR β* , *RASSF1a*, *ER β* , and *TIG1* may be suitable for this unmet need as each has been correlated with known prognostic factors for primary prostate cancer, such as tumor stage and/or Gleason grade (22–25, 59). Indeed in 1 study, *PTGS2* methylation marks in the localized prostate cancer predicted prostate cancer recurrence after radical prostatectomy, independently of tumor stage and Gleason grade (60). In addition, the detection of DNA with *GSTP1* CpG-island hypermethylation in serum of men with localized prostate cancer, where *GSTP1* was also methylated, was associated with an increased risk of prostate cancer recurrence after radical prostatectomy (61). However, we find that prostate cancer patients in which *GSTP1* remains unmethylated have a poorer prognosis and therefore may aid in prediction of prostate cancer recurrence after radical prostatectomy, independently of tumor stage and Gleason grade.

References

1. Ferlay J, Autier P, Boniol M, Heanue M, Colombet M, Boyle P. Estimates of the cancer incidence and mortality in Europe in 2006. *Ann Oncol* 2007;18:581–92.
2. Fitzpatrick JM, Schulman C, Zlotta AR, Schroder FH. Prostate cancer: a serious disease suitable for prevention. *BJU Int* 2009; 103:864–70.
3. Cancer Research UK. Prostate cancer incidence statistics. [cited 2009 September]. Available from: <http://info.cancerresearchuk.org/cancerstats/types/prostate/incidence/>.
4. Short M, Harding J, Christensen E, Conley E. Cancer in Australia: an overview, 2006. Canberra, ACT: Australian Institute of Health and Welfare & Australasian Association of Cancer Registries; 2007.
5. National Cancer Institute Surveillance E, and End Results program. American Cancer Society, Cancer Facts & Figures 2004.
6. Enokida H, Shiina H, Urakami S, et al. Ethnic group-related differences in CpG hypermethylation of the *GSTP1* gene promoter among African-American, Caucasian and Asian patients with prostate cancer. *Int J Cancer* 2005;116:174–81.
7. Holliday R. The inheritance of epigenetic defects. *Science* 1987; 238:163–70.
8. Horner MJ RL, Krapcho M, Neyman N, Aminou R, Howlander N, Altekruse SF, et al., editors. SEER Cancer Statistics Review, 1975–2006. based on November 2008 SEER data submission, posted to the SEER web site, 2009. [cited 2009 September]. Available from: http://seer.cancer.gov/csr/1975_2006/.
9. Landis S, Murray T, Bolden S, Wingo P. Cancer statistics, 1998. *CA Cancer J Clin* 1998;48:6–29.
10. McDavid K, Lee J, Fulton J, Tonita J, Thompson T. Prostate cancer incidence and mortality rates and trends in the United States and Canada. *Public Health Rep* 2004;119:174–86.
11. De Angelis G, Rittenhouse HG, Mikolajczyk SD, Blair Shamel L, Semjonow A. Twenty years of PSA: from prostate antigen to tumor marker. *Rev Urol* 2007;9:113–23.
12. Lin DW. Beyond PSA: utility of novel tumor markers in the setting of elevated PSA. *Urol Oncol* 2009;27:315–21.
13. Schulz WA, Hoffmann MJ. Epigenetic mechanisms in the biology of prostate cancer. *Semin Cancer Biol* 2009;19:172–80.
14. Cooper CS, Foster CS. Concepts of epigenetics in prostate cancer development. *Br J Cancer* 2009;100:240–5.
15. Li LC. Epigenetics of prostate cancer. *Front Biosci* 2007;12:3377–97.
16. Maruyama R, Toyooka S, Toyooka K, et al. Aberrant promoter methylation profile of prostate cancers and its relationship to clinicopathological features. *Clin Cancer Res* 2002;8:514–9.
17. Lee W, Morton R, Epstein J, et al. Cytidine methylation of regulatory sequences near the pi-class glutathione S-transferase gene accompanies human prostatic carcinogenesis. *Proc Natl Acad Sci U S A* 1994;91:11733–7.
18. Okegawa T, Nutahara K, Higashihara E. Association of circulating tumor cells with tumor-related methylated DNA in patients with hormone-refractory prostate cancer. *Int J Urol* 2010;17:466–75.
19. Bastian PJ, Yegnasubramanian S, Palapattu GS, et al. Molecular biomarker in prostate cancer: the role of CpG island hypermethylation. *Eur Urol* 2004;46:698–708.
20. Goericke-Pesch S, Spang A, Schulz M, et al. Recrudescence of spermatogenesis in the dog following downregulation using a slow release GnRH agonist implant. *Reprod Domest Anim* 2009;44 Suppl2:302–8.
21. Nelson WG, De Marzo AM, Yegnasubramanian S. Epigenetic alterations in human prostate cancers. *Endocrinology* 2009;150:3991–4002.
22. Yegnasubramanian S, Kowalski J, Gonzalgo M, et al. Hypermethylation of CpG islands in primary and metastatic human prostate cancer. *Cancer Res* 2004;64:1975–86.
23. Jerónimo C, Henrique R, Hoque M, et al. Quantitative RARbeta2 hypermethylation: a promising prostate cancer marker. *Clin Cancer Res* 2004;10:4010–4.
24. Zhang J, Liu L, Pfeifer G. Methylation of the retinoid response gene *TIG1* in prostate cancer correlates with methylation of the retinoic acid receptor beta gene. *Oncogene* 2004;23:2241–9.

In conclusion, we have shown for the first time that concordant promoter methylation of *EN1* and *SCTR* genes, which reside in the LRES 2q14.2 region, have a high predictive value for determining cancer from normal tissue and provide a regional panel of novel epigenetic biomarkers to be used in combination with *GSTP1* methylation for increasing the specificity of prostate cancer detection.

Disclosure of Potential Conflicts of Interest

No potential conflicts of interest were disclosed.

Grant support

This work is supported by Cancer Institute NSW (CINSW) program (S. J. Clark), CINSW Fellowship (M.W. Coolen and S. Henshall), and CINSW Student (A.L. Statham) grants and National Health and Medical Research Council (NHMRC) project (427614, 481347), NHMRC fellowship grants (S.J. Clark and R.L. Sutherland) and the Spanish Ministry of Science and Innovation (SAF2008/1409 and CSD2006/49). The acquisition and processing of clinical material and database is supported by an NHMRC Program Grant (#535903) and the RT Hall Trust.

The costs of publication of this article were defrayed in part by the payment of page charges. This article must therefore be hereby marked advertisement in accordance with 18 U.S.C. Section 1734 solely to indicate this fact.

Received July 6, 2010; revised October 20, 2010; accepted November 6, 2010; published OnlineFirst November 23, 2010.

25. Zhu X, Leav I, Leung Y, et al. Dynamic regulation of estrogen receptor-beta expression by DNA methylation during prostate cancer development and metastasis. *Am J Pathol* 2004;164:2003-12.
26. Yamanaka M, Watanabe M, Yamada Y, et al. Altered methylation of multiple genes in carcinogenesis of the prostate. *Int J Cancer* 2003;106:382-7.
27. Bastian P, Ellinger J, Wellmann A, et al. Diagnostic and prognostic information in prostate cancer with the help of a small set of hypermethylated gene loci. *Clin Cancer Res* 2005;11:4097-106.
28. Baden J, Green G, Painter J, et al. Multicenter evaluation of an investigational prostate cancer methylation assay. *J Urol* 2009;182: 1186-93.
29. Frigola J, Song J, Stirzaker C, Hinshelwood R, Peinado M, Clark S. Epigenetic remodeling in colorectal cancer results in coordinate gene suppression across an entire chromosome band. *Nat Genet* 2006;38:540-9.
30. Mayor R, Casadomé L, Azuara D, et al. Long-range epigenetic silencing at 2q14.2 affects most human colorectal cancers and may have application as a non-invasive biomarker of disease. *Br J Cancer* 2009;100:1534-9.
31. Song M, Song S, Ayad N, et al. The tumour suppressor RASSF1A regulates mitosis by inhibiting the APC-Cdc20 complex. *Nat Cell Biol* 2004;6:129-37.
32. Stirzaker C, Song JZ, Davidson B, Clark SJ. Transcriptional gene silencing promotes DNA hypermethylation through a sequential change in chromatin modifications in cancer cells. *Cancer Res* 2004;64:3871-7.
33. Quinn DI, Henshall SM, Haynes AM, et al. Prognostic significance of pathologic features in localized prostate cancer treated with radical prostatectomy: implications for staging systems and predictive models. *J Clin Oncol* 2001;19:3692-705.
34. Clark S, Statham A, Stirzaker C, Molloy P, Frommer M. DNA methylation: bisulphite modification and analysis. *Nat Protoc* 2006;1:2353-64.
35. Rand K, Ho T, Qu W, et al. Headloop suppression PCR and its application to selective amplification of methylated DNA sequences. *Nucleic Acids Res* 2005;33:e1127.
36. Coolen M, Statham A, Gardiner-Garden M, Clark S. Genomic profiling of CpG methylation and allelic specificity using quantitative high-throughput mass spectrometry: critical evaluation and improvements. *Nucleic Acids Res* 2007;35:e119.
37. Horvath LG, Henshall SM, Kench JG, et al. Membranous expression of secreted frizzled-related protein 4 predicts for good prognosis in localized prostate cancer and inhibits PC3 cellular proliferation in vitro. *Clin Cancer Res* 2004;10:615-25.
38. Liu P, Ramachandran S, Ali Seyed M, et al. Sex-determining region Y box 4 is a transforming oncogene in human prostate cancer cells. *Cancer Res* 2006;66:4011-9.
39. Millar DS, Ow KK, Paul CL, Russell PJ, Molloy PL, Clark SJ. Detailed methylation analysis of the glutathione S-transferase pi (GSTP1) gene in prostate cancer. *Oncogene* 1999;18:1313-24.
40. Guldborg P, Worm J, Gronbaek K. Profiling DNA methylation by melting analysis. *Methods* 2002;27:121-7.
41. Clark SJ, Statham A, Stirzaker C, Molloy PL, Frommer M. DNA methylation: bisulphite modification and analysis. *Nat Protoc* 2006;1:2353-64.
42. Schlesinger Y, Straussman R, Keshet I, et al. Polycomb-mediated methylation on Lys27 of histone H3 pre-marks genes for de novo methylation in cancer. *Nat Genet* 2007;39:232-6.
43. Nonn L, Ananthanarayanan V, Gann PH. Evidence for field cancerization of the prostate. *Prostate* 2009;69:1470-9.
44. Coolen MW, Stirzaker C, Song JZ, et al. Consolidation of the cancer genome into domains of repressive chromatin by long-range epigenetic silencing (LRES) reduces transcriptional plasticity. *Nat Cell Biol* 2010;12:235-46.
45. Moon R, Kohn A, De Ferrari G, Kaykas A. WNT and beta-catenin signalling: diseases and therapies. *Nat Rev Genet* 2004;5:691-701.
46. Adamska M, MacDonald B, Sarmast Z, Oliver E, Meisler M. En1 and Wnt7a interact with Dkk1 during limb development in the mouse. *Dev Biol* 2004;272:134-44.
47. Tang C, Biemond I, Lamers C. Expression of peptide receptors in human endocrine tumours of the pancreas. *Gut* 1997;40:267-71.
48. Reis F, Luisi S, Carneiro M, et al. Activin, inhibin and the human breast. *Mol Cell Endocrinol* 2004;225:77-82.
49. Mylonas I, Jeschke U, Shabani N, Kuhn C, Friese K, Gerber B. Inhibin/activin subunits (inhibin-alpha, -betaA and -betaB) are differentially expressed in human breast cancer and their metastasis. *Oncol Rep* 2005;13:81-8.
50. Ting AH, McGarvey KM, Baylin SB. The cancer epigenome—components and functional correlates. *Genes Dev* 2006;20:3215-31.
51. Widschwendter M, Fiegl H, Egle D, et al. Epigenetic stem cell signature in cancer. *Nat Genet* 2007;39:157-8.
52. Xiang Y, Zhu Z, Han G, Lin H, Xu L, Chen CD. JMJD3 is a histone H3K27 demethylase. *Cell Res* 2007;17:850-7.
53. Varambally S, Dhanasekaran SM, Zhou M, et al. The polycomb group protein EZH2 is involved in progression of prostate cancer. *Nature* 2002;419:624-9.
54. Gal-Yam EN, Egger G, Iniguez L, et al. Frequent switching of Polycomb repressive marks and DNA hypermethylation in the PC3 prostate cancer cell line. *Proc Natl Acad Sci USA* 2008;105: 12979-84.
55. Rosenbaum E, Hoque M, Cohen Y, et al. Promoter hypermethylation as an independent prognostic factor for relapse in patients with prostate cancer following radical prostatectomy. *Clin Cancer Res* 2005;11:8321-5.
56. Enokida H, Shiina H, Urakami S, et al. Multigene methylation analysis for detection and staging of prostate cancer. *Clin Cancer Res* 2005;11:6582-8.
57. Berezovska OP, Glinskii AB, Yang Z, Li XM, Hoffman RM, Glinsky GV. Essential role for activation of the Polycomb group (PcG) protein chromatin silencing pathway in metastatic prostate cancer. *Cell Cycle* 2006;5:1886-901.
58. Flori AR, Steinhoff C, Muller M, et al. Coordinate hypermethylation at specific genes in prostate carcinoma precedes LINE-1 hypomethylation. *Br J Cancer* 2004;91:985-94.
59. Liu L, Yoon J, Dammann R, Pfeifer G. Frequent hypermethylation of the RASSF1A gene in prostate cancer. *Oncogene* 2002; 21:6835-40.
60. Yegnasubramanian S, Kowalski J, Gonzalgo ML, et al. Hypermethylation of CpG islands in primary and metastatic human prostate cancer. *Cancer Res* 2004;64:1975-86.
61. Bastian P, Palapattu G, Lin X, et al. Preoperative serum DNA GSTP1 CpG island hypermethylation and the risk of early prostate-specific antigen recurrence following radical prostatectomy. *Clin Cancer Res* 2005;11:4037-43.
62. Zhao W, Soejima H, Higashimoto K, et al. The essential role of histone H3 Lys9 di-methylation and MeCP2 binding in MGMT silencing with poor DNA methylation of the promoter CpG island. *J Biochem* 2005;137:431-40.